

# fatigue analysis at filled hole locations – an analytical approach

Over the recent past, material scientists and engineers have started developing custom made structures from composite materials in order to obtain desired mechanical, electrical, magnetic, thermal, optical, and environmental properties.



**Satya Iyengar**  
QuEST Global

**Vinay Rao**  
QuEST Global

# contents

|     |                          |       |
|-----|--------------------------|-------|
| 1.0 | Abstract                 | 03    |
| 2.0 | Introduction             | 03-04 |
| 3.0 | Fatigue Scenarios        | 04    |
| 4.0 | Fatigue Spectrum         | 05-06 |
| 5.0 | Analysis Procedure       | 07    |
| 6.0 | SN Curves for Composites | 07-12 |
| 7.0 | Limitations              | 12    |
| 8.0 | Scope for Future Work    | 13    |
| 9.0 | Conclusion               | 13    |
| 10  | Author Profile           | 13-14 |
| 11  | About QuEST Global       | 14    |



## Abstract

Over the recent past, material scientists and engineers have started developing custom made structures from composite materials in order to obtain desired mechanical, electrical, magnetic, thermal, optical, and environmental properties.

Because of the above advantages, composites have, over the recent past, been used in progressively greater quantities in the aerospace industry. Boeing's 787 Dreamliner and Airbus A350 are among the new generation of commercial aircrafts that use composite materials extensively.

The weight of aircraft components made of composite materials is reduced by approximately 20%, such as in the case of the 787 Dreamliner [1].

Although bonded joints of composite materials have been shown to have very high theoretical efficiency in literature, the preferred method of joining structures in aircrafts is by using bolted or riveted joints. The number of fasteners in an aircraft runs into millions. For example, there are a few hundred thousand rivets or bolts in a pair of A350 wings.

This white paper seeks to address the issues and challenges faced by the aerospace industry in quantifying these composite fastened joints for fatigue conditions.

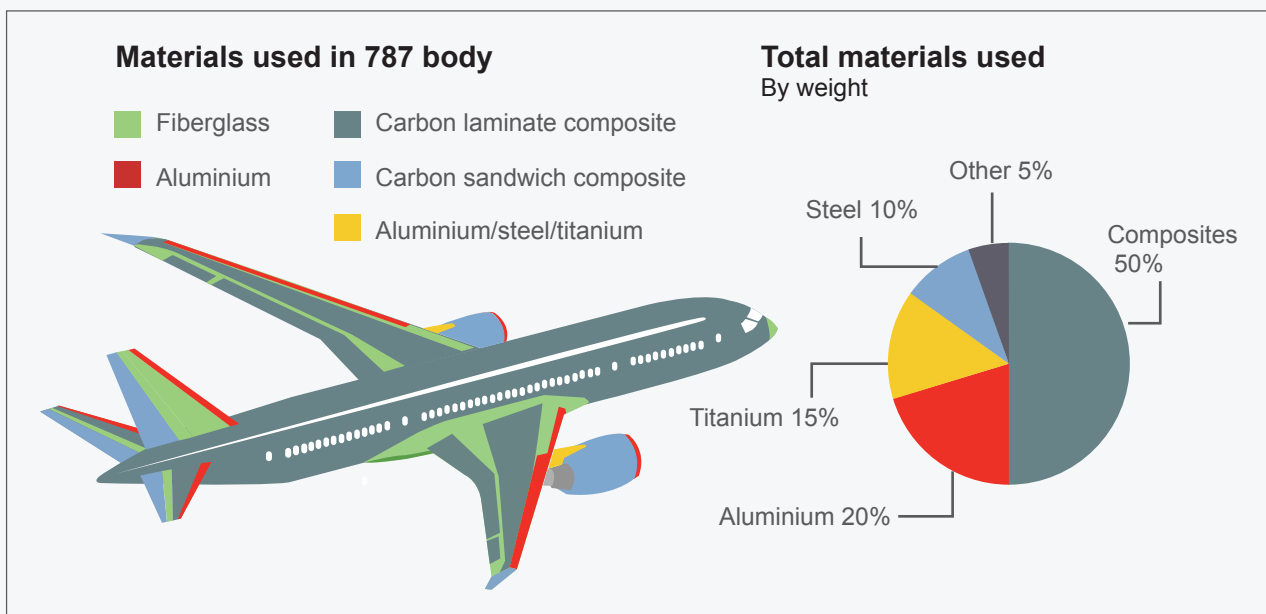


Figure 1: Materials Used in Boeing 787 Body [1]

## Introduction

As with all other materials, composites are also prone to failure. The failure analysis of composites is quite a challenge as they are anisotropic and heterogeneous in nature.

Great strides have been made in the development of analytical and empirical models to substantiate composite materials for static loading conditions. This has largely reduced the need to test composites under static loading.

Also, the general belief is that composite materials are not prone to fatigue failure. However, in aerospace applications, composites are seldom without stress concentrations, and stress concentrations would inherently act as nuclei for crack initiation.

A thorough knowledge of the fatigue behavior of composites is very important for proper design and optimization of structures for use in the aerospace industry. The prevalent practice is to certify a composite structure based on evidence from structural testing.

However, experimental prediction of the fatigue behavior of various composites under different failure modes is prohibitively expensive, as there are unlimited combinations of matrix type, fiber type, and stacking sequences possible.

In this paper, an approach is presented to determine the fatigue life of composites used in aircraft structures with filled holes acting as stress concentrations.

In order to use the approach, while it is recognized that some coupon testing may be necessary, the advantage of the approach is that it utilizes commonly available analytical/empirical rules prevalent in generic F&DT analyses to determine the RFs at any filled hole location. Also, this simple methodology can be automated in a tool and can be easily used to determine the fatigue criticality of a composite structure at fastener locations.

## Fatigue Scenarios

Most primary structures in an aircraft, which are nowadays being manufactured using composite laminates, have unavoidable geometric discontinuities that lead to stress concentrations.

These stress concentrations act as crack nucleation sites. Listed below are some of the common stress concentrations:

- 1) Filled Holes (fastener locations) – These locations are subjected to bearing/bypass stresses
- 2) Corners (in C-sections spars, etc.) – The corners are subjected to inter-laminar tension and shear stresses

- 3) Open Holes (window cut-outs in the fuselage skins, etc.) – These locations are subjected to field stresses

This paper mainly focuses on the substantiation of filled holes for composite fatigue. It is generally believed that in composite materials, after crack initiation, there is a rapid propagation resulting in catastrophic failure. Furthermore, the various temperature changes that aircraft structures are subjected to causes them to be subjected to thermal fatigue.

It has to be noted that the structure should be designed in such a way that there is no crack initiation during the entire Design Service Objective (DSO).

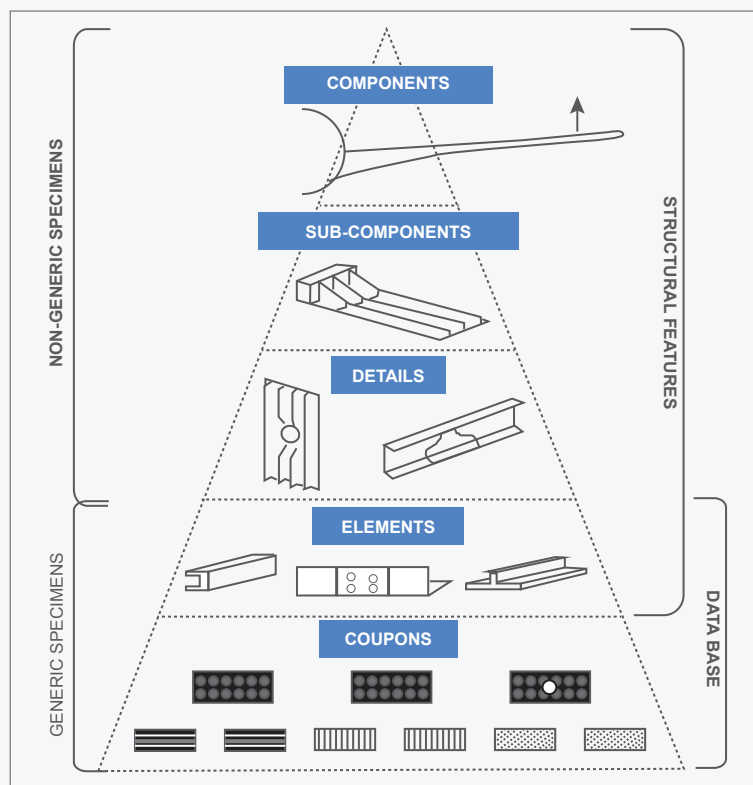


Figure 2: Building-Block Approach Showing the Pyramid of Tests Used for Structural Substantiation [2]



## Fatigue Spectrum

Commercial aircrafts are designed to operate in the following nine missions:

|                            | TROPICAL | POLAR | STANDARD DAY |
|----------------------------|----------|-------|--------------|
| Short Range Mission (SRM)  | ✓        | ✓     | ✓            |
| Medium Range Mission (MRM) | ✓        | ✓     | ✓            |
| Long Range Mission (LRM)   | ✓        | ✓     | ✓            |

Table 1: Mission Mix of Commercial Aircrafts

The GAG cycle for each of the missions can be broadly broken down as shown below:

| SRM (75 to 100 Min) | MRM (270 to 330 Min) | LRM (660 to 750 Min) |
|---------------------|----------------------|----------------------|
| Ground              | Ground               | Ground               |
| Take-off            | Take-off             | Take-off             |
| Climb               | Climb 1              | Climb 1              |
|                     | Cruise 1             | Cruise 1             |
| Cruise              | Climb 2              | Climb 2              |
|                     | Cruise 2             | Cruise 2             |
| Descent             | Descent              | Descent              |
| Approach            | Approach             | Approach             |
| Landing             | Landing              | Landing              |

Table 2: GAG Segments for Various Missions

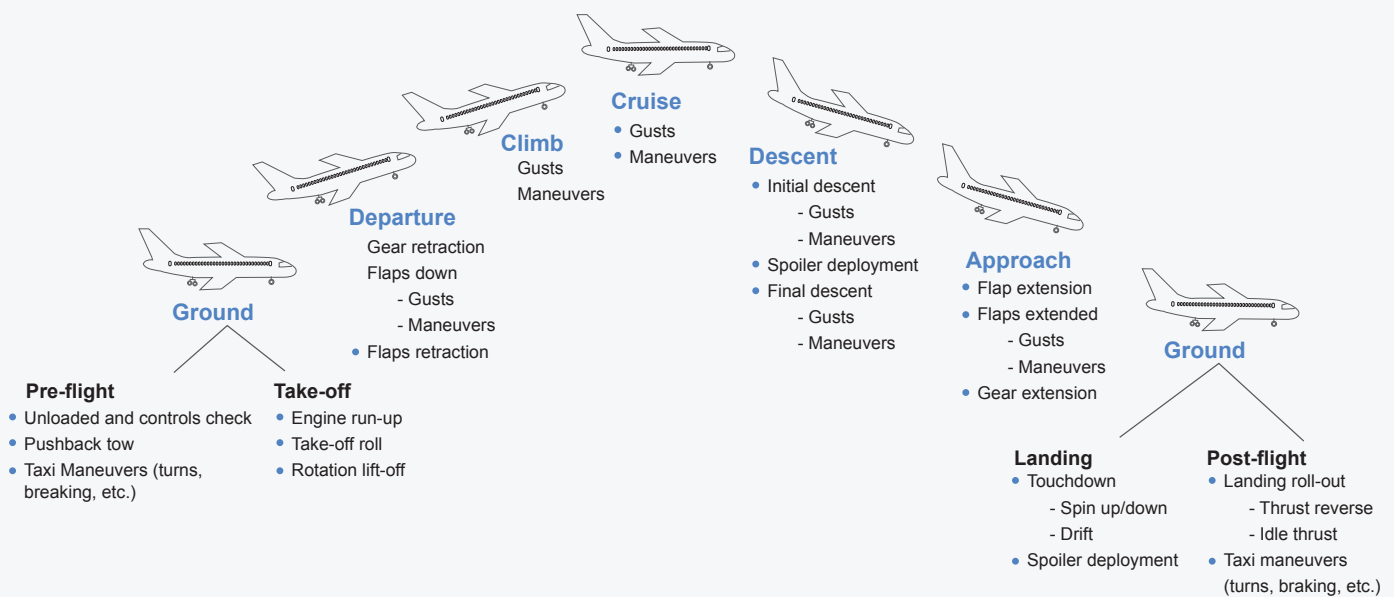


Figure 3: Schematic Representation of a GAG Cycle



In each of the above segments, there will be incremental cases. Some typical incremental loads are listed in Table 3.

| GAG Flight Segment | Mechanical Incremental Cases            | Thermal Condition (@ fuselage as an example) (assembly temperature 23 degrees C) |          |             |
|--------------------|---|--|----------|-------------|
|                    |   | Polar  | Standard | Tropical    |
| Ground             | Towing                                  | Cold   | Hot      | Hot         |
|                    | Pushback/Spring-back                    |  |          |             |
|                    | Turn (slow/medium speed and high speed) |  |          |             |
|                    | Pre-flight Braking                      |  |          |             |
|                    | Bump during taxi-out                    |  |          |             |
| Take-off           | Bump During Take-off run                | Cold   | Hot      | Hot         |
| Climb              | Rotation                                | Cold   | Cold     | Hot to Cold |
|                    | Vertical gust                           |  |          |             |
|                    | Lateral Gust                            |  |          |             |
| Cruise             | Coordinated Turn                        | Cold   | Cold     | Cold        |
|                    | Vertical gust                           |  |          |             |
|                    | Lateral Gust                            |  |          |             |
| Approach/Descent   | Rotation                                | Cold   | Cold     | Cold to Hot |
|                    | Vertical gust                           |  |          |             |
|                    | Lateral Gust                            |  |          |             |
| Landing            | MLG Touch Down                          | Cold   | Hot      | Hot         |
|                    | Bump after touch down                   |  |          |             |
|                    | Turn (slow/medium speed and high speed) |  |          |             |
|                    | Post Flight braking                     |  |          |             |
|                    | Bump during taxi-out                    |  |          |             |

Table 3: Incremental Loads and Temperature Conditions at Various GAG Segments

These mechanical 1g and incremental cases, combined with the thermal loads at various segments of the GAG, result in a “Thermo-Mechanical spectrum” of fatigue stresses.

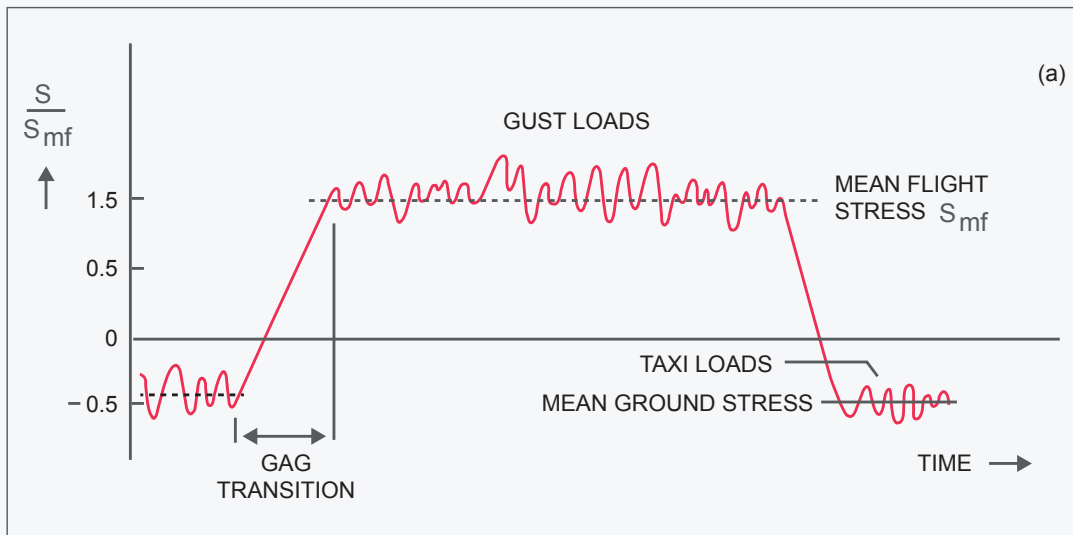


Figure 4: Example Flight Stress History [3]



## Analysis Procedure

Consider a composite to composite joint, as shown below:

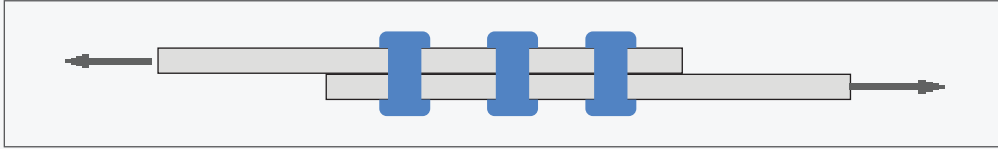


Figure 5: Schematic Representation of a Composite Joint

Each bolt in this joint is subjected to the in-plane bearing/bypass stresses as shown below:

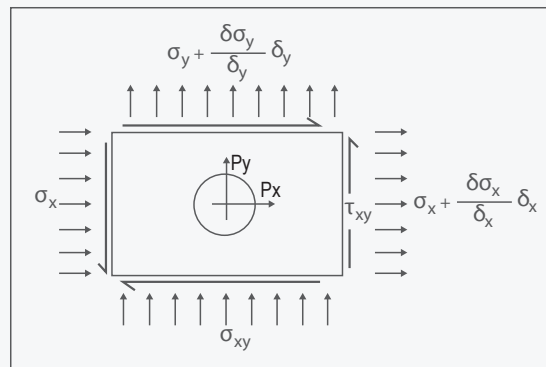


Figure 6: Stress State at a Fastener Location

In order to analyze the bolt for fatigue, a “thermo-mechanical mix spectrum” of all these stresses has to be determined, i.e., the bearing and bypass stresses for the various 1g and incremental load cases corresponding to the various missions has to be determined.

However, the coupon test-based S-N curve will generally be based on field stresses. In order to compare with the test based S-N curve, we have to generate a spectrum of field stresses.

## SN Curves for Composites

SN curves can be used for composite material analysis, with certain salient features as explained below.

### The Ordinate

Since infinite number of laminates can be developed using any given lamina, the SN curves for composites are “normalized” by expressing the ordinate as a “percentage of mean static strength”. By doing so, the SN curves for any particular lamina can be used for most

laminates developed from that lamina material. The mean static strength can be determined from standard coupon testing, based on the prevalent ASTM standards (ex: ASTM D 6742/D 6742 M – 07 for filled hole tension and compression testing)

Figure 7 shows an example of normalized SN curves of the field stresses for three sample laminae, which has to be developed through a coupon test program.

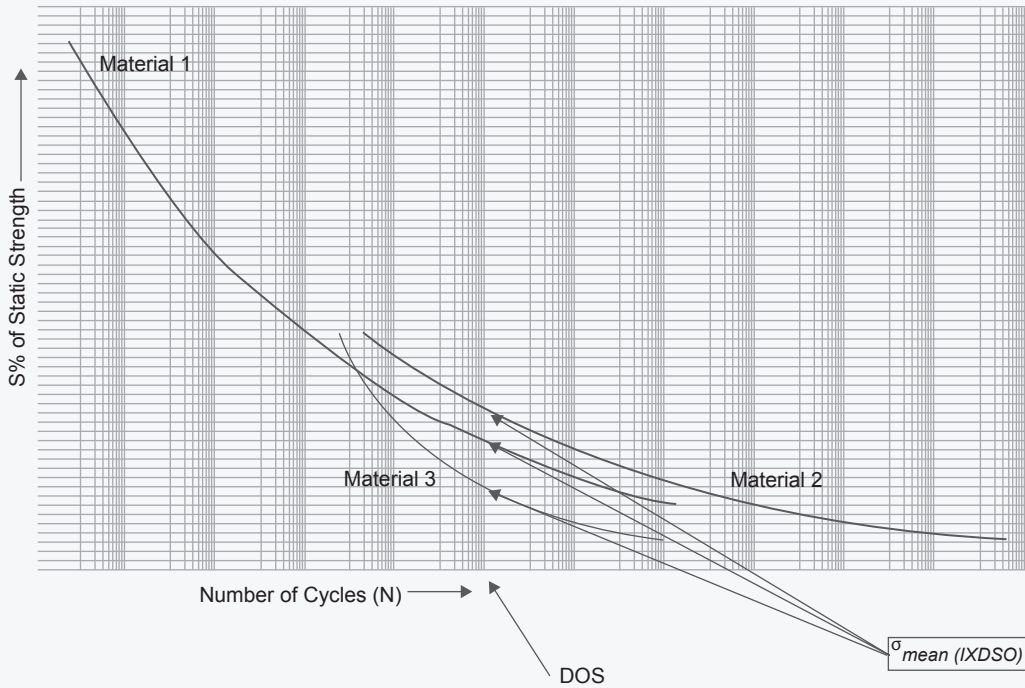


Figure 7: Example Normalized SN Curve of the Field Stresses for Three Sample Lamina Materials

**R Ratio**

In general, the testing for composite fatigue is done at an R ratio (ratio of minimum stress to maximum stress) of -1. This is because unlike in metallics, compressive stresses adversely affect fatigue life of composites.

**Normalization of Applied Spectrum**

Since each cycle of the local stress spectrum is compared to a “normalized” SN curve, the local stress

spectrum shall be normalized too. Thus the local stress spectrum is divided by the mean static strength and multiplied by 100.

$$\text{Normalized local stress spectrum stresses} = \frac{\text{Applied Local Spectrum Stresses}}{\text{Mean Static Strength}} * 100$$

In order to determine a spectrum of field stresses, the bearing stresses need to be converted into an “equivalent far-field stress”, so that it can be added to any existing bypass stress, as shown below.

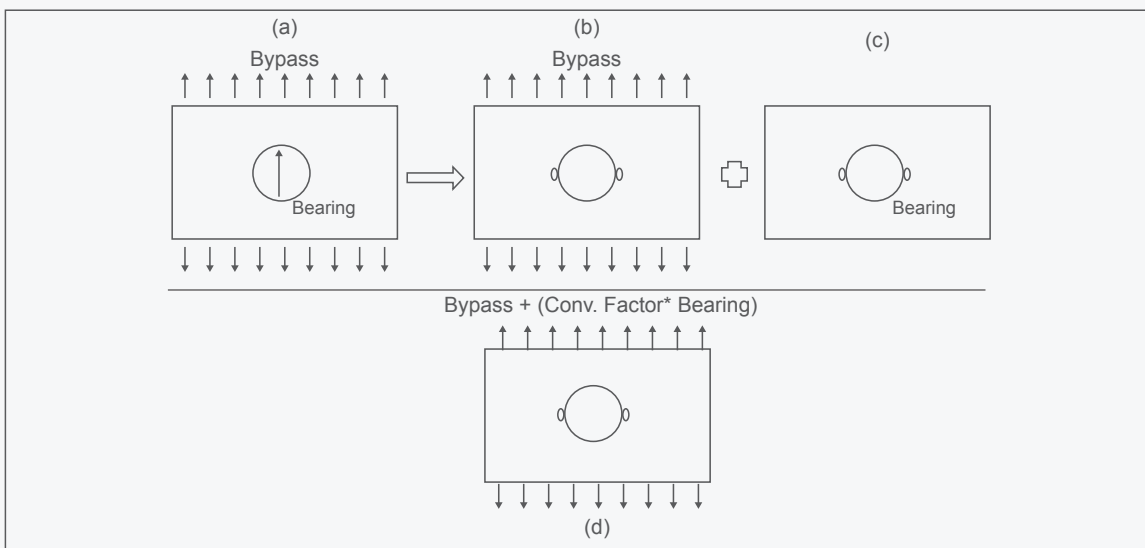


Figure 8: Conversion of Bearing to Equivalent Bypass

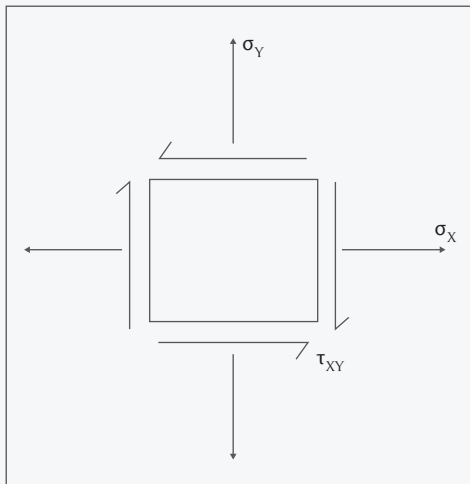


Any finite element software can be used to determine the conversion factor to convert bearing stresses into an “equivalent far-field stress”, using relevant stress concentration factors.

Figure 8 (a) shows a composite filled hole location subjected to bearing and bypass stresses. In Figure 8 (b), the stress concentration due to bypass is schematically shown (at the 3 O’ Clock and 6 O’ Clock positions). Under bearing stresses, the stress concentration at the 12 O’ Clock position is shown in Figure 8 (c). However, using any finite element software, the stress concentration due to bearing at the 3 O’ Clock and 6 O’ Clock positions can be determined, and an “equivalent bypass” can be determined for the applied bearing stress. Figure 8 (d) shows the equivalent field stress, i.e., the applied bypass and the “equivalent bypass” due to the applied bearing stress.

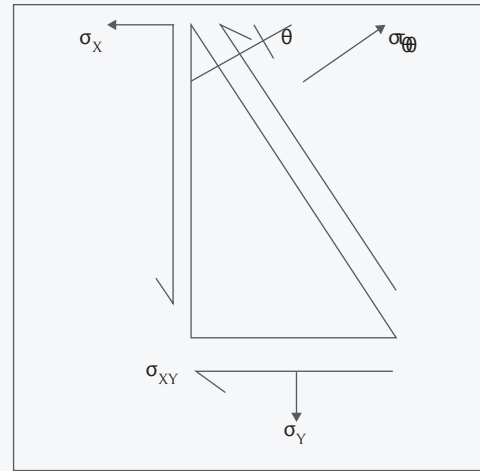
Once the spectrum of field stresses (as shown in Figure 8 (d)) is generated, an “equivalent strain based resolved stress” is determined as explained below:

Determination of resolved stress from the 2D stress state



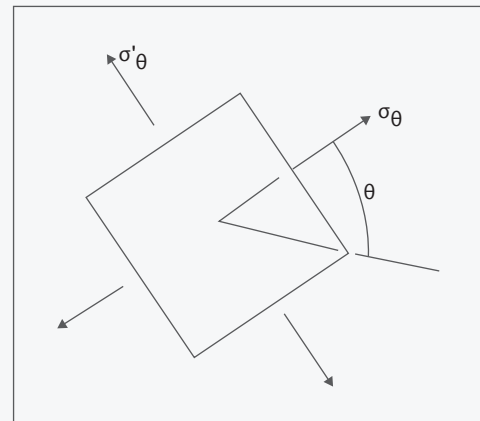
Once the stresses state shown in Figure 6 is converted to a state containing only bypass stresses (shown in adjacent sketch), the three stresses  $\sigma_x$ ,  $\sigma_y$  and  $\tau_{xy}$  can be resolved by the transformation equations into stresses on a plane at  $(\theta+90)$  degrees from x-axis.

$$\sigma_{\theta} = \frac{\sigma_x + \sigma_y}{2} + \frac{\sigma_x - \sigma_y}{2} \cos 2\theta + \tau_{xy} \sin 2\theta \quad (1)$$



$$\tau_{\theta} = \frac{\sigma_x - \sigma_y}{2} \sin 2\theta + \tau_{xy} \cos 2\theta \quad (2)$$

Eq. (1) can be further transformed to give the biaxial stresses on an element at angle  $\theta$ .



$$\sigma_{\theta} = \sigma_x \cos^2 \theta + \sigma_y \sin^2 \theta + \tau_{xy} \sin 2\theta \quad (3)$$

$$\sigma_{\theta'} = \sigma_x \sin^2 \theta + \sigma_y \cos^2 \theta - \tau_{xy} \sin 2\theta \quad (4)$$

Note that unless  $\sigma_{\theta}$  and  $\sigma_{\theta'}$  are principal stresses, there will still be a shear stress present on the element. However shear stresses do not (for small deformations) contribute to direct strain and so are ignored.

The direct strain in the direction of  $\sigma_{\theta}$  is

$$\varepsilon_{\theta} = \frac{\sigma_{\theta}}{E} - \nu_{12} \frac{\sigma_{\theta'}}{E} \quad (5)$$

where  $\nu$  = Poisson’s ratio

This is the strain due to the biaxial system of stresses. Consider the same strain in a uniaxial stress field. A ‘strain equivalent’ stress is given by



$$\sigma_{\epsilon} = \epsilon_{\theta} E = \sigma_{\theta} - \nu_{12} \sigma'_{\theta} \quad (6)$$

$$\sigma_{\epsilon} = \sigma_x \cos^2 \theta + \sigma_y \sin^2 \theta + \tau_{xy} \sin 2\theta - \nu_{12} (\sigma_x \sin^2 \theta + \sigma_y \cos^2 \theta - \tau_{xy} \sin 2\theta)$$

$$\sigma_{\epsilon} = (\sigma_x - \nu_{12} \sigma_y) \cos^2 \theta + (\sigma_y - \nu_{12} \sigma_x) \sin^2 \theta + (1 + \nu_{12}) \tau_{xy} \sin 2\theta \quad (7)$$

Substituting from eq. (3) and (4)

The fatigue RF is determined by following the below process.

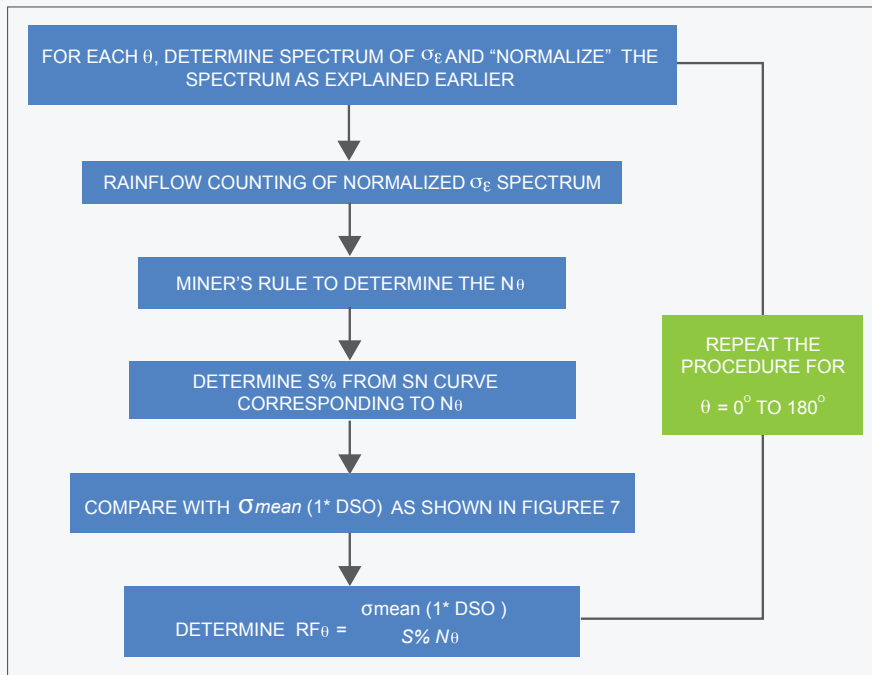


Figure 9: Flowchart to Determine Fatigue RF

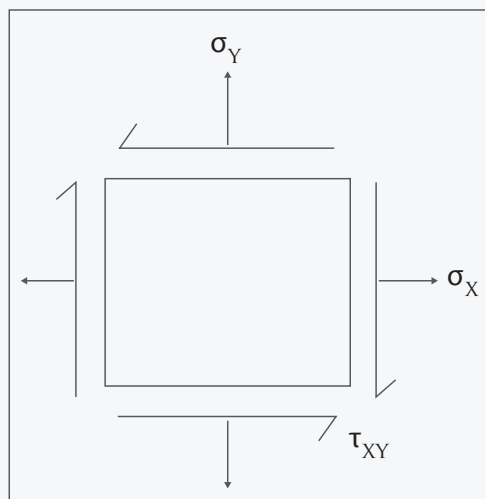
RF = Min (RF01, RF02, RF03,.....).

Max Damage Angle =  $\theta$  corresponding to RF Illustrative Example

For example, consider a composite joint under a stress state shown in the adjacent sketch.

Let us assume a composite to be made by stacking layers of lamina with a normalized curve for field stresses as shown below in Figure 10.

For the given stress state, a strain equivalent stress  $\sigma_{\epsilon}$  can be determined for various  $\theta$  values, for various 1g and incremental cases, so that a spectrum of  $\sigma_{\epsilon}$ - $\theta$  for each  $\theta$  is obtained.



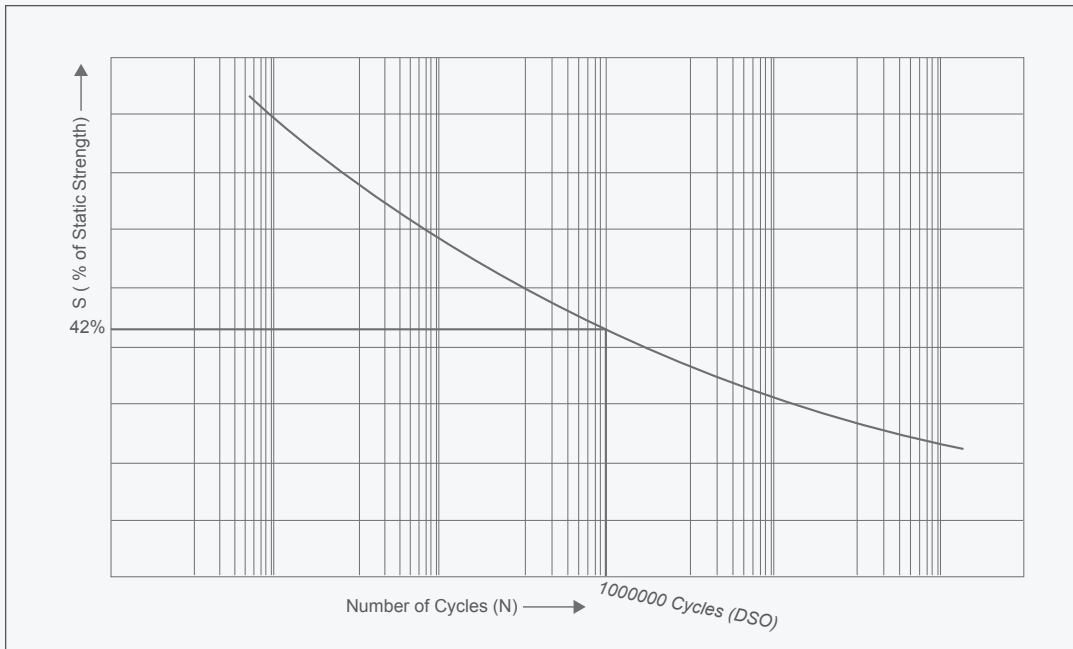


Figure 10: Example Normalized SN Curve for the Material ( $\sigma_{mean}(1*DSO) = 42\%$ )

Post-processing the spectrum using the rainflow counting technique, the  $N_\theta$  can be determined corresponding to each  $\sigma_\epsilon$ - $\theta$  spectrum. Using the results

of the rainflow counting and the normalized SN curves, the  $RF_\theta$  can be determined for various  $\theta$  values, as shown in Table 4 and Figure 11.

| $\theta$ | Raw Data Post Processed Using Rainflow Counting Algorithm |       | $N_\theta$ from Miner's Rule | $\sigma_{EQ}$ (S% from SN Curve) | $\sigma_{mean}(1*DSO)$ (%) | $RF_\theta$ |
|----------|---|-------|------------------------------|----------------------------------|----------------------------|-------------|
| 0        | $\sigma_\epsilon$ -0-1                                    | N0-1  | 17000000                     | 35.5                             | 42                         | 1.18        |
|          | $\sigma_\epsilon$ -0-2                                    | N0-2  |                              |                                  |                            |             |
|          | $\sigma_\epsilon$ -0-3                                    | N0-3  |                              |                                  |                            |             |
|          | -   | -     |                              |                                  |                            |             |
|          | $\sigma_\epsilon$ -0-n                                    | N0-n  |                              |                                  |                            |             |
| 45       | $\sigma_\epsilon$ -45-1                                   | N45-1 | 200000000                    | 30                               | 42                         | 1.40        |
|          | $\sigma_\epsilon$ -45-2                                   | N45-2 |                              |                                  |                            |             |
|          | $\sigma_\epsilon$ -45-5                                   | N45-5 |                              |                                  |                            |             |
|          | -   | -     |                              |                                  |                            |             |
|          | $\sigma_\epsilon$ -45-n                                   | N45-n |                              |                                  |                            |             |
| 90       | $\sigma_\epsilon$ -90-1                                   | N90-1 | 1000000000                   | 27.7                             | 42                         | 1.52        |
|          | $\sigma_\epsilon$ -90-2                                   | N90-2 |                              |                                  |                            |             |
|          | $\sigma_\epsilon$ -90-3                                   | N90-3 |                              |                                  |                            |             |
|          | -   | -     |                              |                                  |                            |             |
|          | $\sigma_\epsilon$ -90-n                                   | N90-n |                              |                                  |                            |             |

Table 4: Illustration of the Process in Figure 9

\* - All data presented in the table is for illustration purposes only In Table 4



- $\sigma_{\epsilon-\theta-n}$  is the strain equivalent stress (eq. (7)) and  $N_{\theta-n}$  is the number of cycles at the corresponding stress level. This data is obtained by applying the Rainflow Counting algorithm to the normalized spectrum of the strain equivalent stress  $\sigma_{\epsilon}$  corresponding to an angle of resolution  $\theta$
- $N_{\theta}$  can be obtained after rainflow counting using the relation:

$$\frac{1}{N_{\theta}} = \frac{1}{N_{\theta-1}} + \frac{1}{N_{\theta-2}} + \frac{1}{N_{\theta-3}} + \dots + \frac{1}{N_{\theta-n}} \quad (8)$$

- $\sigma_{EQ}$  for each  $\theta$  value can be obtained from the SN Curve, as shown in Figure 11.
- $\sigma_{mean}(1*DSO) = 42\%$ , as shown in Figure 11

$$RF_{\theta} = \frac{\sigma_{mean}(1*DSO)}{\sigma_{EQ-\theta}}$$

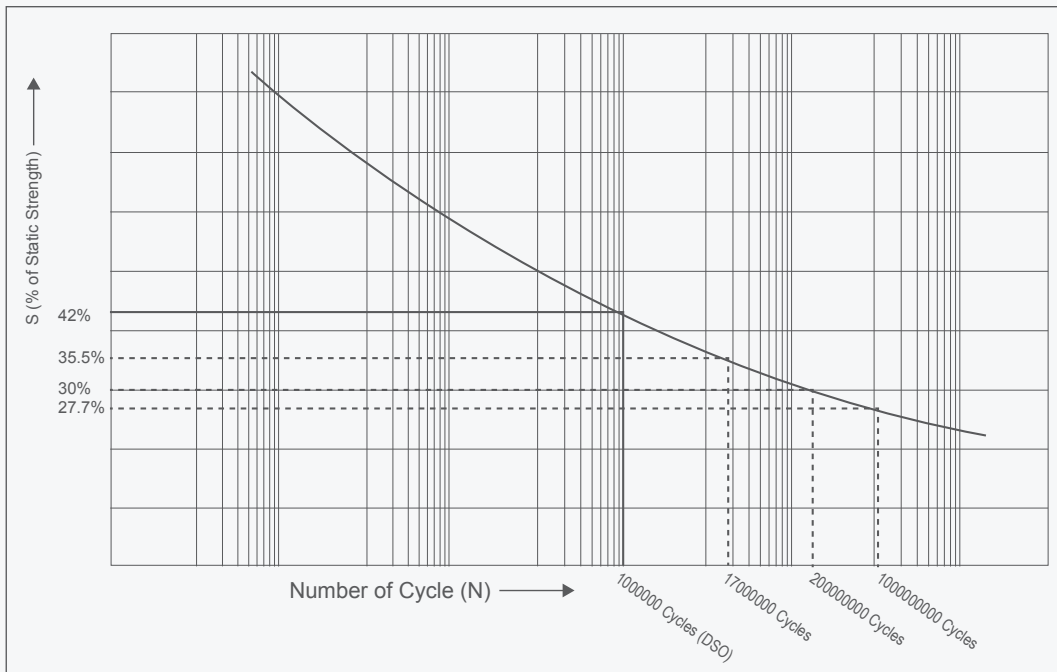


Figure 10: Example Normalized SN Curve for the Material ( $\sigma_{mean}(1*DSO) = 42\%$ )

As can be seen from Table 4,  $RF_{\theta}$  is minimum for  $\theta = 0^{\circ}$ . Hence,

Maximum damage angle =  $0^{\circ}$   
 $RF = 1.18$

## Limitations

This approach can only be applied in the presence of material specific normalized SN curves corresponding to the failure mode. It is imperative that a coupon test program is undertaken to develop the curves. The test program needs to be adequately extensive, and needs to include parametric studies to study the effects of laminate thickness, hole diameter, environmental conditioning etc., so that appropriate knockdown factors could be used as and when applicable.

Certain assumptions are necessary if this approach has to be used for filled hole locations, such as determination of an “equivalent bypass” flow corresponding to a given bearing load. A complete understanding of the time history is a pre-requisite before the application of this methodology. Automation is necessary to perform repetitive, time consuming calculations such as rainflow counting. This approach is applicable only for laminated composites, and cannot be used for sandwich structures.



## Scope for Future Work

A set of normalized SN curves can be developed for the most commonly used laminae in aircrafts for future references. Also, parametric studies can be performed and knockdown factors can be developed by generating SN curves using coupons of different diameters, and at various environmental conditions.

Similar methodologies can be developed for other commonly occurring failure modes in composite aircraft structures, such as corner unfolding, buckling etc.

Another closely related topic to the fatigue behavior of composite laminates is the residual strength analysis of laminates, which has not been discussed in this paper. Further studies that will be able to relate the effect of mean static strength, the predicted life from normalized SN curves and the residual strength of laminates will be able to provide a thorough understanding.

## Conclusion

The high use of fastener joints, combined with the shift towards more composite structures in modern aircrafts demands an efficient way to quantify the fastener locations for fatigue failure. The methodology presented in this paper can be used to determine fatigue reserve factors at fastener locations with minimum need for testing. The approach can also be suitably used for open hole locations such as penetrations and cut outs. The maximum damage angle can also be determined from this approach, and is a useful input during joint design.

## References

- 1) [http://www.appropedia.org/Composites\\_in\\_the\\_Aircraft\\_Industry](http://www.appropedia.org/Composites_in_the_Aircraft_Industry)
- 2) Laminate Statistical Allowable Generation for Fiber-Reinforced Composite Materials: Lamina Variability Method, U.S D.O.T, Jan 2009, Tomblin J., Seneviratne, W.
- 3) European Approaches in Standard Spectrum Development, Aalt A. ten Have, Development of Fatigue Loading Spectra, 1989

## Author Profile



### Satya Iyengar

Satya Iyengar is Chief Engineer, Airbus Wing and Pylon Design Center at QuEST and is responsible for technical and quality standards of work done in the Airbus ODC. He also provides technical support to the planning and management of projects and work packages and ensures implementation of procedures within the Quality Management System at the ODC.

Satya is also responsible for identifying and initiating training on relevant subjects including knowledge of Airbus tools, methods, and procedures. He has worked extensively on a variety of GKN projects such as the A350 spar corner bending, rib post analysis, EA2, EA3, and EA4 projects, A400M inlet ducts, A400M detailed FEM, A380 FTE, and Concessions on A380, SA, LR aircrafts. Satya holds a B. S. degree in Mechanical Engineering from Bangalore University and an M. S. degree in Mechanical Engineering from the University Of Cincinnati

Email: [info@quest-global.com](mailto:info@quest-global.com)

## Author Profile



### Vinay Rao

Vinay Rao has been with QuEST for over two years now and works as a Lead Engineer at the GKN GDC India Center. He has spent his entire career in the Aerospace industry, mostly working on composite materials and structures and has adequate experience in structural stress analysis as well as coupon and sub-component level composite material testing and qualification.

Vinay is a Mechanical Engineer by qualification, with a Bachelor's degree from VTU, and a Master's degree (specializing in laminated composites) from Wichita State University.

Email: [info@quest-global.com](mailto:info@quest-global.com)

## About QuEST Global

QuEST Global is a focused global engineering solutions provider with a proven track record of over 17 years serving the product development & production engineering needs of high technology companies. A pioneer in global engineering services, QuEST is a trusted, strategic and long term partner for many Fortune 500 companies in the Aero Engines, Aerospace & Defence, Transportation, Oil & Gas, Power, Healthcare and other high tech industries. The company offers mechanical, electrical, electronics, embedded, engineering software, engineering analytics, manufacturing engineering and supply chain transformative solutions across the complete engineering lifecycle.

QuEST partners with customers to continuously create value through customer-centric culture, continuous improvement mind-set, as well as domain specific engineering capability. Through its local-global model, QuEST provides maximum value engineering interactions locally, along with high quality deliveries at optimal cost from global locations. The company comprises of more than 7,000 passionate engineers of nine different nationalities intent on making a positive impact to the business of world class customers, transforming the way they do engineering.



BORN TO ENGINEER

<http://quest-global.com>